J|A|C|S
ARTICLES
Published on Web 03/03/2007

Ultraviolet Resonance Raman Evidence for Utilization of the Heme 6-Propionate Hydrogen-Bond Network in Signal Transmission from Heme to Protein in *Ec* DOS Protein

Samir F. El-Mashtoly,[‡,||] Hiroto Takahashi,[§] Toru Shimizu,[§] and Teizo Kitagawa*[,‡,†]

Contribution from the Okazaki Institute for Integrative Bioscience, National Institutes of Natural Sciences, Okazaki, Aichi 444-8787, Japan, and Institute of Multidisciplinary Research for Advanced Material, Tohoku University, 2-1-1 Katahira, Aoba-ku, Sendai 980-8577, Japan

Received September 28, 2006; E-mail: teizo@ims.ac.jp

Abstract: The direct oxygen sensor protein from *Escherichia coli* (*Ec* DOS) is a heme-based signal transducer protein responsible for phosphodiesterase (PDE) activity. Binding of either O_2 or CO molecule to a reduced heme enhances the PDE activity toward 3′,5′-cyclic diguanylic acid. We report ultraviolet resonance Raman (UVRR) spectroscopic investigations of the reduced, O_2- and CO-bound forms of heme-bound PAS domain of *Ec* DOS. The UVRR results show that heme discriminates different ligands, resulting in altered conformations in the protein moiety. Specifically, the environment around Trp53 that contacts the 2-vinyl group of heme, is changed to a more hydrophobic environment by O_2 binding, whereas it is changed to a more hydrophilic environment by CO-binding. In addition, the PDE activity of the O_2- and CO-bound forms for the Trp53Phe mutant is significantly decreased compared with that of the wild type (WT), demonstrating the importance of Trp53 for the catalytic reaction. On the other hand, the binding of O_2 or CO to the heme produces drastic changes in the Tyr126 of I_β-strand at the surface of the sensor domain. Furthermore, we found that Asn84 forms a hydrogen bond with Tyr126 either in the O_2- or CO-bound forms but not in the reduced form. Finally, the PDE activities of the ligand-bound forms for Asn84Val and Tyr126Phe mutants are significantly reduced as compared with that of WT, suggesting the importance of the hydrogen-bonding network from heme 6-propionate to Tyr126 through Asn84 in signal transmission.

Introduction

A variety of heme-containing gas-sensor proteins have been discovered by gene analysis from bacteria to mammals.[1−6] Heme sensor proteins are indispensable for organisms to survive in fitting to their environment, but the working mechanism remains to be clarified. Generally this kind of proteins is composed of an N-terminal heme-containing sensor domain and a C-terminal catalytic domain. The binding of CO, NO, or O_2 to the heme slightly changes a structure of heme, which alters the protein conformation in the vicinity of the heme, and the conformational change is propagated to the catalytic domain, leading to regulation of the protein activity. The protein activity depends on types of catalytic domains, including protein kinases, guanylate cyclase, phosphodiesterases, and transcriptional activators.

The O_2-sensing proteins identified so far include FixL,[7] phosphodiesterase A1 protein from *Acetobactoer xylinum* (*Ax* PDEA1),[8] direct oxygen sensor (DOS),[9] and HemAT.[10] FixL from *Rhizobium* contains a heme-bound PAS (an acronym formed from the names of proteins in which imperfect repeat sequences were initially recognized: the *Drosophilia* period clock protein (PER), vertebrate aryl hydrocarbon receptor nuclear translocator (ARNT), and *Drosophila* single-minded protein (SIM)) domain as a sensor.[7,11,12] The catalytic domain of FixL serves as a protein kinase that phosphorylates the FixJ protein, which regulates the expression of nitrogen fixation gene. *Ax* PDEA1 has a heme-bound PAS domain as a sensor, and it catalyzes the hydrolysis of 3′,5′-cyclic diguanylic acid (c-di-GMP), which is required for the activation of cellulose synthase in cellulose-producing bacteria. HemAT is the first sensor

[‡] National Institutes of Natural Sciences.
[§] Institute of Multidisciplinary Research for Advanced Material.
[||] Present Address: Department of Physiology and Biophysics, Albert Einstein College of Medicine, Bronx, New York 10461.
[†] Present Address: Toyota Physical & Chemical Research Institute, Nagakute, Aichi 480-1192, Japan.

(1) Rodgers, K. R. *Curr. Opin. Chem. Biol.* **1999**, *3*, 158−167.
(2) Chan, M. K. *Nat. Struct. Biol.* **2000**, *7*, 822−824.
(3) Aono, S.; Nakajima, H. *Coord. Chem. Rev.* **1999**, *190−192*, 267−282.
(4) Gilles-Gonzalez, M.-A.; Gonzalez, G. *J. Inorg. Biochem.* **2005**, *99*, 1−22.
(5) Uchida, T.; Kitagawa, T. *Acc. Chem. Res.* **2005**, *38*, 662−670.
(6) Sasakura, Y.; Yoshimura-Suzuki, T.; Kurokawa, H.; Shimizu, T. *Acc. Chem. Res.* **2006**, *39*, 37−43.
(7) Gilles-Gonzalez, M. A.; Ditta, G. S.; Helinski, D. R. *Nature* **1991**, *350*, 170−172.
(8) Chang, A. L.; Tuckerman, J. R.; Gonzalez, G.; Mayer, R.; Weinhouse, H.; Volman, G.; Amikam, D.; Benziman, M.; Gilles-Gonzalez, M.-A. *Biochemistry* **2001**, *40*, 3420−3426.
(9) Delgado-Nixon, V. M.; Gonzalez, G.; Gilles-Gonzalez, M.-A. *Biochemistry* **2000**, *39*, 2685−2691.
(10) Hou, S.; Larsen, R. W.; Boudko, D.; Riley, C. W.; Karatan, E.; Zimmer, M.; Ordal, G. W.; Alam, M. *Nature* **2000**, *403*, 540−544.
(11) Gong, W.; Hao, B.; Mansy, S. S.; Gonzalez, G.; Gilles-Gonzalez, M. A.; Chan, M. K. *Proc. Natl. Acad. Sci. U.S.A.* **1998**, *95*, 15177−15182.
(12) Nakamura, H.; Kumita, H.; Imai, K.; Iizuka, T.; Shiro, Y. *Proc. Natl. Acad. Sci. U.S.A.* **2004**, *101*, 2742−2746.

10.1021/ja0669777 CCC: $37.00

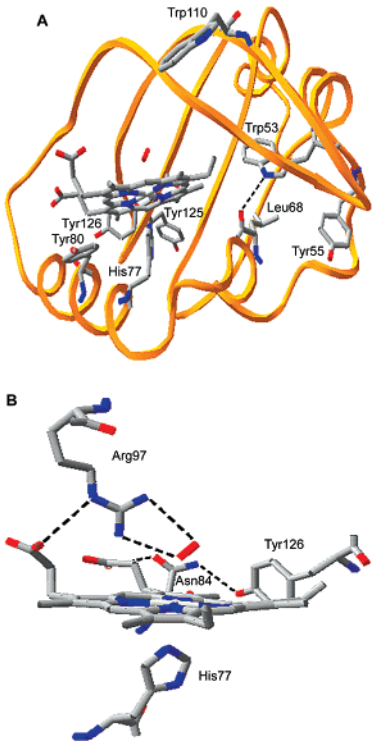

Figure 1. X-ray structure of the O_2-bound *Ec* DOSH protein (PDB ID: 1S66; ref 18). The heme and Trp, Tyr, Leu68, and His77 residues are shown in Figure 1A. Hydrogen-bond networks around iron-bound O_2 and heme propionates of *Ec* DOSH are displayed in Figure 1B.

protein identified with a myoglobin-like fold, and it is involved in aerotaxis of bacteria and archaea.[10,13,14]

The DOS protein from *Escherichia coli* (*Ec* DOS) is a heme-based signal transducer protein responsible for phosphodiesterase (PDE) activity.[9] The *Ec* DOS is composed of an N-terminal heme-bound PAS domain and a C-terminal PDE catalytic domain. *Ec* DOS was initially reported to exhibit PDE activity in a redox and/or O_2 dependent manner.[9,15] In fact, the reduced form of *Ec* DOS yielded the PDE activity toward adenosine 3′5′-cyclic monophosphate (cAMP), but the oxidized, CO- and NO-bound forms were inactive.[15] On the other hand, it is reported recently that the *Ec* DOS protein has a specific PDE activity toward c-di-GMP,[16] and the binding of O_2 or CO to the reduced heme enhances the PDE activity.[17]

Figure 1A displays the crystal structure of the truncated heme sensor domain (*Ec* DOSH) of *Ec* DOS protein. The O_2 and His77 are the heme axial ligands in the distal and proximal sides, respectively.[18] *Ec* DOSH protein contains two Trp and four Tyr residues. Trp53, Tyr80, and Tyr126 are located near the heme peripheral groups, while, Trp110, Tyr55, and Tyr125 are located near the surface of the sensor domain (Figure 1A). Therefore, these residues can be used as probes to monitor the protein conformational changes near and far from the heme (see later).

(13) Hou, S.; Freitas, T.; Larsen, R. W.; Piatibratov, M.; Sivozhelezov, V.; Yamamoto, A.; Meleshkevitch, E. A.; Zimmer, M.; Ordal, G. W.; Alam, M. *Proc. Natl. Acad. Sci. U.S.A.* **2001**, *98*, 9353−9358.
(14) Ohta, T.; Yoshimura, H.; Yoshioka, S.; Aono, S.; Kitagawa, T. *J. Am. Chem. Soc.* **2004**, *126*, 15000−15001.
(15) Sasakura, Y.; Hirata, S.; Sugiyama, S.; Suzuki, S.; Taguchi, S.; Watanabe, M.; Matsui, T.; Sagami, I.; Shimizu, T. *J. Biol. Chem.* **2002**, *277*, 23821−23827.
(16) Schmidt, A. J.; Ryjenkov, D. A.; Gomelsky, M. *J. Bacteriol.* **2005**, *187*, 4774−4781.
(17) Takahashi, H.; Shimizu, T. *Chem. Lett.* **2006**, *35*, 970−971.
(18) Park, H. J.; Suquet, C.; Satterlee, J. D.; Kang, C. *Biochemistry* **2004**, *43*, 2738−2746.

Figure 1B illustrates the hydrogen-bond networks around the iron-bound O_2 and heme propionates of *Ec* DOSH protein. In the O_2-bound form, 7-propionate forms a hydrogen bond with Arg97 that stabilizes the heme-coordinated O_2, while, 6-propionate constitutes a hydrogen-bond network with Asn84 and Tyr126.[18] These hydrogen-bonding systems are candidates for a communication pathway between heme and the protein moiety. In fact, the switching of axial ligand from O_2 to Met95 upon heme reduction perturbs the hydrogen-bonding network starting from 7-propionate, resulting in large conformational changes in the FG turn.[18] On the other hand, the role of the 6-propionate hydrogen-bonding network is not clear in the signal transmission.

To address this issue, we have performed ultraviolet resonance Raman (UVRR) investigations for the reduced, O_2-, and CO-bound forms of *Ec* DOSH protein and several mutants, and examined the enzymatic activities for the full-length *Ec* DOS. We first monitored the conformational changes in wild-type (WT) *Ec* DOSH upon binding of O_2 and CO. We found that heme discriminates between different ligands by inducing significantly altered conformations near Trp53 that contacts heme 2-vinyl group. In addition, the PDE activity of the O_2- and CO-bound forms for W53F mutant is significantly decreased compared with that of WT, demonstrating the importance of Trp53 for the catalytic reaction. On the other hand, the results of several mutants (Y55F, Y80F, Y125F, Y126F, and N84V) suggest that Asn84 forms a hydrogen bond with Tyr126 in the O_2- or CO-bound forms but not in the reduced form. Furthermore, the PDE activities of the ligand bound forms for N84V and Y126F mutants are significantly reduced compared with that of WT, suggesting the importance of the heme 6-propionate hydrogen-bonding network from heme to Tyr126 through Asn84 for signal transmission.

Experimental Section

Sample Preparation. Cloning of *Ec* DOSH, construction of the expression plasmids, and purification of the WT and mutant proteins were performed essentially as described previously.[15] The expression and purification of the full-length *Ec* DOS proteins were performed using slight modifications (Overexpression and Purification of *Ec* DOS in Supporting Information) of previously described procedures.[15] Site-directed mutagenesis was performed by a PCR-based approach as implemented in the QuikChange kit (Stratagene). The purities of *Ec* DOS samples were confirmed to be more than 95% homogeneous by SDS-PAGE.

For Raman measurements, *Ec* DOSH was further purified by gel filtration through Superdex 75 (26/60 cm) pre-equilibrated with 50 mM Tris-HCl buffer at pH 7.5. The concentration of the protein was adjusted to 100 and 300 μM in 50 mM Tris-HCl buffer (pH 7.5) for 229 and 244 nm excitations, respectively. As an internal intensity standard for calculating UVRR difference spectra, 400 and 100 mM sodium sulfate (Na_2SO_4) aliquots were incorporated into the sample solutions for the excitations at 229 and 244 nm, respectively. The oxidized *Ec* DOSH was prepared by adding an excess amount of potassium ferricyanide to the purified protein, and afterward potassium ferricyanide was removed by gel filtration with Sephadex G25. Reduced *Ec* DOSH was prepared by adding a minimum amount of sodium dithionite solution (final concentration 0.5−1 mM) into the protein solution under nitrogen atmosphere. The O_2-bound form of *Ec* DOSH was prepared by passing the dithionite-reduced *Ec* DOSH protein through a small Sephadex G25 column under an aerobic condition, and then flushing the sample with pure oxygen gas in a sealed Raman cell to obtain 100% saturation.

The CO-adduct of *Ec* DOSH was prepared by incubating the dithionite-reduced *Ec* DOSH with CO-saturated buffer.

UV Resonance Raman Measurements. UV resonance Raman spectra were obtained by using instrumentation described in details previously.[19] The Raman excitation lights at 229 and 244 nm were generated by an intracavity frequency-doubled Ar^+ ion laser (Innova 300 FReD; coherent). The second harmonic in the laser output was separated from the fundamental with a Pellin-Broca prism and focused into a protein sample solution. About a 150 μL aliquot of the sample solution was placed into a spinning cell with a stirring function.[19] Raman scattered light at right angle was collected with a UV microscope objective lens, dispersed with a 126 cm single monochromator (Spex 1269) equipped with a 3600 groove/mm holographic grating, and detected by an intensified charge-coupled device (Princeton Instruments, model ICCD-1024MG-E/1). We adopted spectral resolutions of 7.8 and 6.9 cm^{-1} for the spectra excited at 229 and 244 nm, respectively. The laser power at the sample point was 0.3 mW. The protein sample was replaced with a fresh one every 5−10 min, and the total exposure time to get one spectrum was about 1 h. The integrity of the sample after exposure to UV laser light was carefully confirmed by comparing the visible absorption spectra obtained before and after the UVRR measurements. If some spectral changes were recognized, the Raman spectrum was discarded. Raman shifts were calibrated with cyclohexane, trichloroethylene, 1,2-dichloroethane, and toluene.

Catalytic Activities. Catalytic activities of the full length *Ec* DOS were determined using a colorimetric assay for free phosphate. Catalytic activities were measured at 25 °C under anaerobic conditions (O_2 concentration less than 10 ppm) in a glovebox. The reactions were carried out in a 50 μL reaction mixture containing 50 mM Tris-HCl (pH 8.0), 50 mM NaCl, 5 mM $MgCl_2$, 0.1 mM 3′,5′-cyclic diguanylic acid, 1.5 U CIAP (Takara Bio, Otsu, Japan), and 0.2 μM *Ec* DOS. After the reaction was terminated by 1 N HCl, the solution was centrifuged for 5 min at 15000g. The supernatant (100 μL) was mixed with 200 μL of Biomol Green (Biomol, Plymouth Meeting, PA), and the mixture was incubated at 25 °C for 30 min. The change in absorbance at 630 nm was monitored with a Benchmark Microplate Reader (Bio-Rad, Hercules, CA) and used to determine the phosphate concentration by comparison with a standard curve. To confirm that the heme complex was stable during the catalytic measurement, the optical absorption spectra of the gas-free complexes were always monitored under the exactly the same conditions as those of the activity measurements. We confirmed that no spectral change of the heme occurred during the activity measurements.

Results

Changes in the 229 nm Excited UVRR Spectrum of WT *Ec* DOSH upon Ligand Binding. Raman bands arising from Trp and Tyr residues are selectively enhanced upon excitation around 220−250 nm and can be used as the structural probes for their surroundings.[20,21] Figure 2 shows the raw 229-nm-excited UVRR spectrum of the O_2-bound (a) form of WT *Ec* DOSH and the difference spectra, the reduced−oxidized (b), reduced−CO (c), and reduced−O_2 (d) for WT. The raw spectrum of WT is dominated by the bands arising from two Trp (Trp53 and Trp110) and four Tyr (Tyr55, Tyr80, Tyr125, and Tyr126) residues, which are labeled W and Y, respectively, followed by their mode numbers.[20] Because the protein concentrations are the same in all measurements performed at a given excitation wavelength, the intensities of the Raman features were comparable in all of the raw spectra. The difference spectra were calculated so that the band for SO_4^{2-} (981 cm^{-1}), which was present at the same concentration in all samples as an internal intensity standard, would be zero.

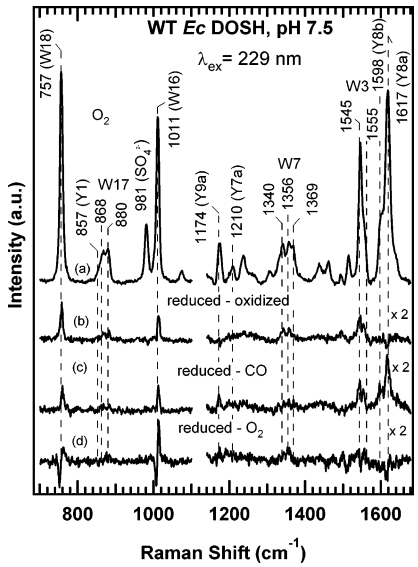

Figure 2. The 229-nm excited UVRR spectra of the WT *Ec* DOSH. Shown are the raw spectrum for the O_2-bound form of the WT (a) and the following difference spectra for WT: (b) reduced−oxidized, (c) reduced−CO, and (d) reduced−O_2.

Difference spectrum b yields positive peaks at 757 (W18), 868/880 (W17), 1011 (W16), 1340/1356 (W7), and 1545/1555 cm^{-1} (W3) bands, indicating an increase in the intensity of the Trp bands in the reduced form compared with the oxidized form. The reduced−CO spectrum difference spectrum (c) displays positive features for Trp bands similar to those observed for heme redox difference (b). In addition, spectrum c reveals positive peaks at 1174 (Y9a), 1598 (Y8b), and 1617 cm^{-1} (Y8a), indicating a decrease in the intensity of the Tyr bands upon CO binding. On the other hand spectrum d exhibits negative/positive peaks at 752/763 and 1006/1014 cm^{-1}, which are produced from a frequency downshift of W18 and W16 vibrations upon O_2 binding, respectively. Furthermore, spectrum d displays small features for W7, W3, and Y8a bands. Thus, the UVRR difference spectra demonstrate that the Trp and Tyr Raman bands experience spectral changes upon CO-binding different from those observed upon O_2-binding.

Spectral Changes of Trp Induced by O_2 Binding in the 229 nm Excited Spectra. Figure 3 displays the raw UVRR spectra of the O_2-bound form for WT (a), W110I (b), and W53F (c) excited at 229 nm and reduced−O_2 difference spectra for WT (d), W110I (e), and W53F (f). The frequency of W17 band (~875 cm^{-1}) is known to serve as a marker of hydrogen bonding of the Trp indole ring.[22,23] The W17 bands of WT (a) and Trp53 (in W110I) (b) are observed as a doublet at 868 and 880 cm^{-1}, which correspond to the strongly hydrogen-bonded and non-hydrogen-bonded Trp residues,[22] respectively (see also Figure S1 in Supporting Information). Although the crystal structure shows that Trp53 forms a hydrogen bond with Leu68,[18] in solution at least, it is more likely that Trp53 occupies two

(19) Aki, M.; Ogura, T.; Shinzawa-Itoh, K.; Yoshikawa, S.; Kitagawa, T. *J. Phys. Chem. B* **2000**, *104*, 10765−10774.
(20) Harada, I.; Takeuchi, H. In *Spectroscopy of Biological Systems*; Clark, R. J. H., Hester, R. E., Eds.; Advances in Spectroscopy 13; John Wiley & Sons: Chichester, U.K., 1986; pp 113−175.
(21) Austin, J. C.; Jordan, T.; Spiro, T. G. In *Biomolecular Spectroscopy, Part A*; Clark, R. J. H., Hester, R. E., Eds.; Advances in Spectroscopy 20; John Wiley & Sons: Chichester, U.K., 1993; pp 55−127.
(22) Miura, T.; Takeuchi, H.; Harada, I. *Biochemistry* **1988**, *27*, 88−94.
(23) Takeuchi, H. *Biopolymers* **2003**, *72*, 305−317.

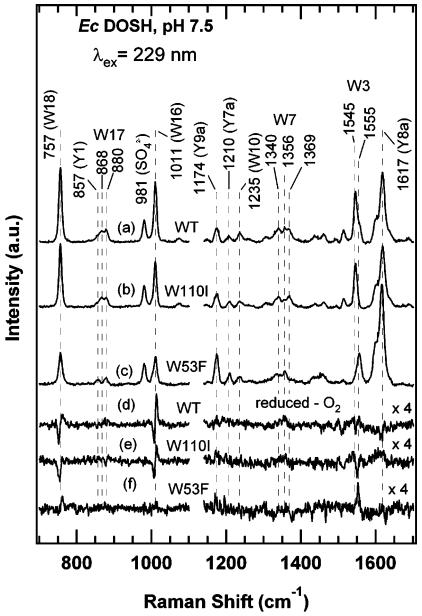

Figure 3. The 229-nm excited UVRR spectra of WT and Trp mutants of *Ec* DOSH. Shown are the raw spectra for the O_2-bound form of WT (a), W110I (b), and W53F (c) and the reduced−O_2 difference spectra for WT (d), W110I (e), and W53F (f) mutants.

different conformations. On the other hand, Trp110 is solvent exposed (Figure 1A) and is expected to interact with water molecules. However, the W17 frequency of W53F (880 cm^{-1}, Figure 3c) suggests that Trp110 does not form a hydrogen bond in the O_2-bound form.

The W7 band of Trp usually splits into a doublet at 1360/1340 cm^{-1} owing to Fermi resonance between a fundamental mode at 1340 cm^{-1} and a combination of two out-of-plane modes involving the benzene and pyrrole rings comprising the Trp side chain.[20,21,23] The W7 band of WT (Figure 3a), however, exhibits an unusual triplet feature with an additional peak at 1369 cm^{-1} (see also Figure S1 in Supporting Information). A similar triplet has been observed for Trp53 of W110I (Figure 3b), while a doublet at 1339/1357 cm^{-1} is observed for Trp110 of W53F (Figure 3c). Thus, the high-frequency component at 1369 cm^{-1} in WT spectrum (a) is assigned to Trp53.

The frequency of Trp W3 mode is sensitive to the absolute value of torsion angle, $|\chi^{2,1}|$ about the $C_\beta-C_3$ bond connecting the indole ring to the peptide main chain.[24] The W3 mode of WT (Figure 3a and Figure S1 in Supporting Information) has a main peak at 1545 cm^{-1} with a shoulder at 1555 cm^{-1}. The W3 frequencies of Trp53 (in W110I, Figure 3b) and Trp110 (in W53F, Figure 3c) at 1545 and 1555 cm^{-1} correspond to the $|\chi^{2,1}|$ angle of 81° and 105°, respectively. X-ray diffraction data show that Trp53 and Trp110 in the O_2-bound form have $\chi^{2,1}$ values of 76 and 98°, respectively.[18] These values are close to those expected from W3 frequencies.

Figure 3d reveals the derivative-like peaks at 752/763 and 1006/1014 cm^{-1}, which are produced from frequency downshifts of W18 and W16 vibrations, respectively, upon O_2 binding. A strong negative peak is observed for Trp53 (in W110I, e) at 752 cm^{-1}, but a weak positive peak is present at 762 cm^{-1} in the spectrum of Trp110 (in W53F, f). Therefore, the derivative peak around 757 cm^{-1} for W18 vibration of WT (spectrum d)

(24) Miura, T.; Takeuchi, H.; Harada, I. *J. Raman Spectrosc.* **1989**, *20*, 667−671.

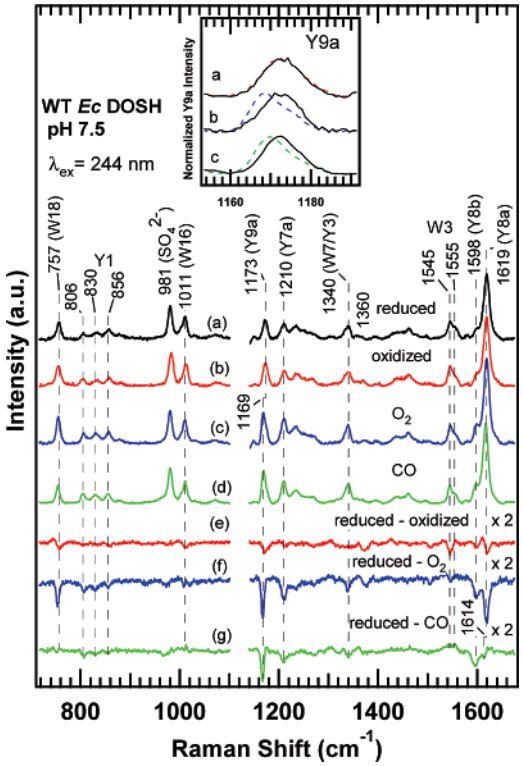

Figure 4. The 244-nm excited UVRR spectra of WT *Ec* DOSH. Spectra shown are the reduced (a), oxidized (b), O_2-bound (c), and CO-bound forms (d) and the following difference spectra: (e) reduced−oxidized, (f) reduced−O_2, and (g) reduced−CO. The inset shows the enlarged raw spectra of the Y9a mode in the intensity normalized spectra. The reduced (solid black line), oxidized (dotted red line), O_2-bound (dotted blue line), and CO-bound forms (dotted green line) are shown.

arises from the different patterns of two Trp residues. In addition, only Trp53 (e) shows a derivative pattern for W16 (1011 cm^{-1}) similar to that observed for WT (d). The complicated feature of W3 vibration for WT in spectrum d would arise from the different contributions from both Trp53 (e) and Trp110 (f). Thus, both Trp53 and Trp110 exhibit spectral changes upon O_2-binding.

Changes in the 244 nm Excited UVRR Spectrum of WT *Ec* DOSH upon Ligand Binding. Figure 4 depicts the 244 nm excited raw UVRR spectra of the reduced (a), oxidized (b), O_2-bound (c), and CO-bound (d) forms and the difference spectra for reduced−oxidized (e), reduced−O_2 (f), and reduced−CO (g). Upon heme oxidation (b), most of Tyr and Trp Raman bands display small spectral changes as can be seen in spectrum e. It reveals positive/negative peaks at 746/760 and 1610/1620 cm^{-1}, which are due to frequency downshifts of W18 and Y8a vibrations, respectively, upon heme reduction. Trace e also shows negative peaks at 1173, 1210, 1545, and 1598 cm^{-1}, which are produced by intensity reduction of Y9a, Y7a, W3, and Y8b bands, respectively, in the reduced form.

Figure 4c demonstrates the dramatic UVRR spectral changes upon O_2 binding, especially about the following points: (i) The most remarkable difference is the intensity enhancement of all Tyr Raman bands including Y1, Y9a, Y7a, Y8b, and Y8a. (ii) Y9a band downshifts by ∼ 4 cm^{-1} (see inset of Figure 4).

These are more clearly seen in the difference spectrum f (reduced−O_2), which reveals negative peaks for Y1, Y9a, Y7a, Y8b, and Y8a. We should note that trace f does not reveal a differential type peak for Y9a, because the frequency downshift

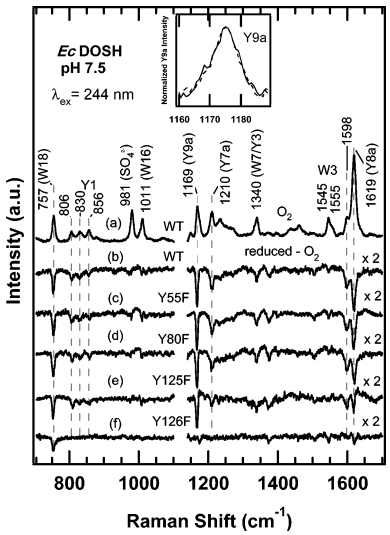

Figure 5. The 244-nm excited UVRR spectra of WT and Tyr mutants of *Ec* DOSH. Shown are the raw spectrum of the O_2-bound WT (a), and the reduced−O_2 difference spectra for WT (b), Y55F (c), Y80F (d), Y125F (e), and Y126F (f). The inset shows the enlarged raw spectra of the Y9a mode in the intensity normalized spectra. The spectra of reduced (solid line) and O_2-bound forms (dotted line) of Y126F mutant are overlain.

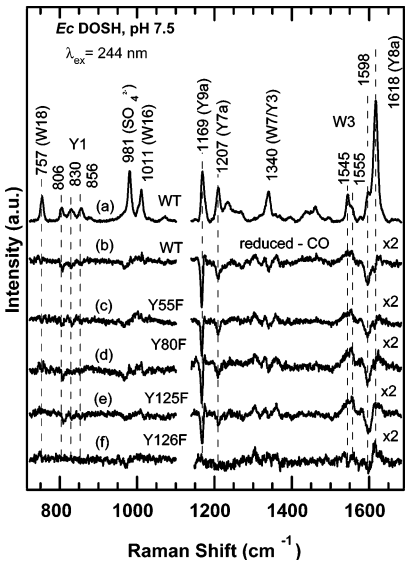

Figure 6. The 244-nm excited UVRR spectra of WT and Tyr mutants of *Ec* DOSH. Shown are the raw spectrum of the CO-bound WT (a), and the reduced−CO difference spectra of WT (b), Y55F (c), Y80F (d), Y125F (e), and Y126F (f).

of the Y9a band is coupled with a large intensity increase upon O_2 binding. Similar spectral changes are observed upon CO binding (d and g). However, spectrum f shows strong negative peaks near 757 and 1619 cm^{-1}, which are due to the intensity enhancement of W18 and Y8a bands upon O_2 binding. On the other hand, spectrum g reveals no change in the W18 band, while a small negative peak is observed at 1614 cm^{-1} (Y8a), upon CO binding. Thus, we conclude that the spectral changes of some Tyr and Trp residues caused by O_2-binding differ from those observed for CO binding.

Specification of Tyr Spectral Changes Induced by O_2 Binding. To assign the spectral changes observed in Figure 4f to a specific Tyr residue, we have measured the raw UVRR spectra of the reduced and O_2-bound forms for Y55F, Y80F, Y125F, and Y126F mutants. Figure 5 displays the raw UVRR spectrum of the O_2-bound form of WT (a) excited at 244 nm and the difference spectra of reduced−O_2 for WT (b), Y55F (c), Y80F (d), Y125F (e), and Y126F (f) of *Ec* DOSH. The difference spectrum for Y55F (c) displays features identical to those observed for the WT (b). This is clearly seen in the double difference spectrum (Figure S2 in Supporting Information) of WT (Figure 5b) and Y55F (Figure 5c), demonstrating that no change occurred in the Tyr55 environment of WT upon O_2 binding.

Although the difference spectra for Y80F (Figure 5d) and Y125F (Figure 5e) exhibit negative peaks for all Tyr Raman bands similar to those of WT (b), the intensity of the negative peak for Y8a (1619 cm^{-1}) is reduced in the spectra of Y80F (d) and Y125F (e). In addition, the intensities of Y9a and Y7a bands are slightly decreased in Y125F (e) (see also Figure S2 in Supporting Information). Thus, both Tyr80 and Tyr125 of F-helix and I_β strand, respectively, experience different environmental changes upon O_2 binding. The UVRR spectra of Y55F, Y80F, and Y125F (Figure 5c−e) show the presence of strong negative peaks at Y1, Y9a, Y7a, Y8b, and Y8a, which are contrasted with those for Y126F (Figure 5f), in which the strong negative peaks of Tyr are absent (or weaker) and also no frequency downshift is observed for the Y9a band upon O_2 binding (see the inset of Figure 5). This strongly suggests that Tyr126 in the WT protein undergoes significant spectral changes upon O_2 binding. Thus, UVRR results indicate that Tyr126 of the I_β strand in WT experiences the largest changes upon O_2-binding, while Tyr80 and Tyr125 residues undergo small environmental changes.

It is known that deprotonation of the Tyr model compound results in large intensity enhancement of all Tyr Raman bands and also frequency downshifts of Y9a and Y8a bands.[20,21,25] Parts of these effects are essentially identical to those seen in Figure 5b. To examine whether these spectral changes arise from deprotonation of Tyr residue upon ligand binding, we have monitored the effect of pH on Y1, Y9a, and Y7a bands of WT as shown in Figure S3 (Supporting Information). The results show that no significant change occurs in the intensity and frequency of Tyr bands as a function of pH. Consequently, we can rule out a possibility of tyrosinate formation in the WT O_2-bound form below pH 9.0.

Specification of Tyr Spectral Changes Induced by CO Binding. Figure 6 depicts the raw UVRR spectrum of the CO-bound form of WT (a) excited at 244 nm and the reduced−CO difference spectra for WT (b), Y55F (c), Y80F (d), Y125F (e), and Y126F (f) of *Ec* DOSH. The difference spectra for Y55F (c) and Y80F (d) show features similar to those observed for the WT (b). However, the negative peak at Y9a is smaller than that observed for WT (b). This is clearly seen in the double difference spectra (Figure S4 in Supporting Information) of WT and Tyr mutants, indicating that the environment around Tyr55 and Tyr80 residues in WT are less significantly altered upon CO binding. In addition, the negative feature at 1614 cm^{-1} for WT spectrum (Figure 6b) is absent in Y125F spectrum (Figure 6e). The intensity of the negative peak of Y9a is also reduced in Y125F spectrum (e). Thus, Tyr125 of the I_β strand experiences environmental changes upon CO-binding. Furthermore, most of the strong negative peaks in the WT spectrum (b)

(25) Nagai, M.; Aki, M.; Li, R.; Jin, Y.; Sakai, H.; Nagatomo, S.; Kitagawa, T. *Biochemistry* **2000**, *39*, 13093−13105.

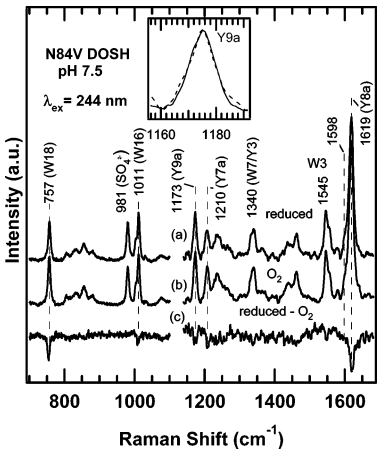

Figure 7. The 244-nm excited UVRR spectra of N84V mutant of *Ec* DOSH. Shown are the raw spectra of the reduced (a) and O_2-bound (b) forms of the N84V mutant and the reduced−O_2 difference spectrum (c) of the N84V mutant. The inset shows the enlarged raw spectra of the Y9a mode in the intensity normalized spectra. The reduced (solid line) and O_2-bound forms (broken line) of the N84V mutant are overlain.

disappeared or became weaker in the Y126F spectrum (f). These results indicate that Tyr126 undergoes large environmental changes upon CO-binding in the WT form. Therefore, the UVRR results show that Tyr126 exhibits the largest change while other Tyr residues experience more or less environmental changes upon CO binding. We note that a positive peak appears at 1614 cm^{-1} in the Y126F (f) spectrum instead of a small negative peak in spectra (b−d), which arises from Tyr125. Thus, the mutation of Tyr126 residue may perturb the Tyr125 environment.

Changes in N84V Mutant upon O_2 Binding. Generally the formation or breaking of the Tyr hydrogen bond with the surroundings significantly influences the intensity and frequency of Tyr bands.[26,27] Asn84 from F-helix forms hydrogen bonds with both carboxyl terminus of heme 6-propionate and hydroxyl group of Tyr126 (Figure 1B). The changes in the hydrogen-bonding interaction of Asn84 and Tyr126 may be the origin of the observed spectral changes for Tyr126 upon dissociation of O_2 (Figure 4f). To examine this idea, we have performed UVRR investigation of N84V mutant in which the hydrogen bond between Asn84 and Tyr126 is broken. Figure 7 displays the raw UVRR spectra of the reduced (a) and O_2-bound (b) forms for N84V mutant of *Ec* DOSH and the reduced−O_2 difference spectrum (c) for N84V mutant. The spectrum c reveals very small negative peaks at Y9a and Y7a compared with WT spectrum (Figure 4f). The intensity of Y8a band (Figure 7c) is also smaller than that of WT (Figure 4f). In addition, no significant frequency downshift is observed for Y9a band of N84V mutant upon O_2 binding (see inset of Figure 7). Thus, most of the spectral changes observed for Tyr126 upon binding/dissociation of O_2 are absent in N84V mutant. These results strongly suggest that the hydrogen bond between Asn84 and Tyr126 in the WT is present only in the O_2-bound form.

PDE Activity. The present UVRR results of *Ec* DOSH demonstrated that Trp53, Asn84, and Tyr126 experience large environmental changes especially upon ligand binding. To examine the importance of these residues for the catalytic reaction, we prepared the full-length mutants for these residues; W53F, N84V, and Y126F. Their PDE activities were investigated under anaerobic conditions, and the results are summarized in Table 1. Both the oxidized and reduced forms of WT have appreciable PDE activity toward c-di-GMP. The activity is remarkably enhanced by the binding of either O_2 or CO to heme for the reduced form.[17] The PDE activities of reduced and oxidized forms are comparable for W53F, and it is also true for the Y126F mutant. Binding of O_2 or CO to W53F and Y126F mutants only slightly enhances the activity. On the other hand, the PDE activity of the N84V mutant is slightly enhanced upon oxidation of heme, but the activities are little altered by the O_2- and CO-binding to the reduced form.

Table 1. Comparison of the PDE Activities for WT and Mutants

	activity[a]			
mutation	Fe(III)	Fe(II)	Fe(II)–O_2	Fe(II)–CO
WT	4.9	4.3	19.2	18.5
W53F	3.7	4.5	6.8	6.6
N84V	10.1	6.7	6.2	9.9
Y126F	2.7	3.6	ND[b]	9.6

[a] In terms of nmol phosphate/nmol DOS/min. The activities were calculated from the average slope of the linear region of the turnover versus time curves. Each curve included at least three points and gave an $R2 > 0.90$. [b] Not determined (ND) because the Y126F mutant was unstable under the reaction conditions.

Furthermore, it is evident from Table 1 that the reduced and oxidized forms of all the mutants exhibited PDE activities comparable to that of the WT except for the N84V mutant, which yielded slightly higher values. Thus, the cleavage of the hydrogen bond between heme 6-propionate and Asn84 (Figure 1B) in the N84V mutant perturbs the PDE activity in both the reduced and oxidized states. On the other hand, the PDE activity for all the mutants is significantly reduced (by 46−68%) upon the binding of either CO or O_2 to the heme. Thus, the removal of the hydrogen bond between Trp53 and Leu68 in W53F, between heme 6-propionate and Asn84 in N84V, and between Asn84 and Tyr126 in Y126F (Figure 1) significantly perturbs the activity enhancement of the WT upon ligand binding. Therefore, our data clearly demonstrate that Trp53, Asn84, and Tyr126 residues are essential for communication between heme and catalytic site toward c-di-GMP.

Discussion

Conformational Changes of Trp Residues upon Ligand Binding. *Ec* DOSH protein contains two Trp residues, Trp53 and Trp110. Trp53 is located in the C-helix near the heme 2-vinyl group, while Trp110 is located in H_β strand at the surface (Figure 1A). In the present study the two Trp residues are used to probe the tertiary structure changes of protein conformation upon ligand binding. The UVRR results demonstrate that both Trp53 and Trp110 undergo intensity changes of Raman bands upon O_2 binding. In addition, they exhibit an intensity change in the oxidized and CO-bound forms as indicated by positive peaks for W3 bands, which are located at 1545 and 1555 cm^{-1} for Trp53 and Trp110, respectively (Figure 2b−c). The intensities of Trp bands are known to be sensitive to environmental hydrophobicity and/or hydrogen-bonding interactions of the indole side chain.[26,28,29] Since a frequency shift is not observed

(26) Rodgers, K. R.; Su, C.; Subramaniam, S.; Spiro, T. G. *J. Am. Chem. Soc.* **1992**, *114*, 3697−3709.
(27) Takeuchi, H.; Watanabe, M.; Satoh, Y.; Harada, I. *J. Raman Spectrosc.* **1989**, *20*, 233−237.
(28) Chi, Z.; Asher, S. A. *J. Phys. Chem. B* **1998**, *102*, 9595−9602.

for the hydrogen bond marker band (W17 at 868 cm^{-1}), the hydrogen bond between Trp53 and Leu68 hardly changes upon ligand binding. In addition, the W17 vibration of W53F mutant (880 cm^{-1}) suggests that Trp110 does not form a hydrogen bond in any ligand-bound forms.

Therefore, it is reasonable to conclude that the hydrophobicity around Trp53 and Trp110 residues changes upon ligand binding. However, the hydrophobicity changes around Trp53 upon O_2 and CO binding seem to be dissimilar. For instance, the intensity of Trp53 Raman bands is decreased in the CO form but is increased in the O_2-bound form. These results suggest that the environment around Trp53 changes to more hydrophobic in the O_2-bound form whereas to more hydrophilic in the CO-bound form.[28] On the other hand, the intensity of Trp110 band is reduced in both the CO, and O_2-bound forms, implying that the environment around Trp110 changes to more hydrophilic in the CO- and O_2-bound forms. Similar to the CO-bound form, the environments around Trp53 and Trp110 change to more hydrophilic in the oxidized than in the reduced form. However, the crystal structures showed no significant structural changes about Trp53 and Trp110 upon ligand binding or upon redox change.[18,30] This means that UVRR spectroscopy reflects more delicate changes than those found in X-ray crystallographic analysis.

Since Trp53 is located near a heme 2-vinyl group (Figure 1A), the hydrophobicity change around Trp53 is probably produced from an alteration in the interactions of the 2-vinyl group and the surrounding residues. Consistent with this idea, the visible excited RR spectra of WT *Ec* DOSH indicate that the 2-vinyl group vibrations exhibit large spectral changes upon O_2-binding and these changes are perturbed by the W53F mutation (not shown). Furthermore, the conformational change of Trp53 is quite important, because Trp53 is located near the Glu59−Lys104 salt bridge at the surface of the sensor domain.[18] This salt bridge is well conserved on the surface of the PAS domain proteins, and it was proposed that the salt bridge plays an important role in the signal transduction.[31] The reported feature is compatible with the PDE activity for the O_2- or CO-bound forms of the W53F mutant, revealed in the present study; the activity of the W53F mutant is reduced by ∼65% compared to that of the WT.

Conformational Changes of Tyr Residues upon Ligand Binding. *Ec* DOSH protein contains four Tyr residues, Tyr55, Tyr80, Tyr125, and Tyr126. Tyr55 is located in the CD region, while Tyr80 from F-helix is located near the propionate side chains of heme (Figure 1A). Tyr125 and Tyr126 from the I_β sheet lie on the surface of the sensor domain.[18] In addition, Tyr126 forms a hydrogen bond with Asn84 that engages a hydrogen bond with the 6-propionate of heme in the O_2-bound form (Figure 1B). The UVRR results show that Tyr residues experience small spectral changes upon the redox change but larger changes upon ligand binding, indicating the occurrence of large environmental changes. Specifically, Tyr126 on the I_β sheet exhibits the largest environmental change upon O_2 and CO binding, while Tyr80 and Tyr125 from the F-helix and I_β sheet, respectively, experience smaller changes. In addition, Tyr55 undergoes appreciable changes upon the CO-binding, while no significant change upon O_2 binding (Figures 5 and 6).

It was clarified from the model compound studies that the intensity and frequency of Tyr bands are influenced by the formation or cleavage of the hydrogen bond.[26,27] So, we examined the possibility that the changes in the hydrogen-bonding interaction between Asn84 and Tyr126 (Figure 1B) is the origin of the observed spectral changes for Tyr126 upon ligand binding/dissociation. The UVRR results of N84V mutant (Figure 7), in which the hydrogen bond between Tyr126 and Asn84 is absent, reveal smaller changes for almost all Tyr Raman bands compared with those observed for the WT. These results strongly suggest that the absence of the hydrogen bond between Tyr126 and Asn84 is the reason for little spectral change in the N84V mutant and that the hydrogen bond between Tyr126 and Asn84 is the origin of the spectral changes observed for the WT upon O_2 dissociation.

Consequently, we conclude for the first time that the hydrogen bond between Asn84 and the hydroxyl group of Tyr126 in the WT is absent in the reduced form but is formed by O_2 binding, implying that the hydrogen-bonding network from the 6-propionate of heme is altered upon O_2 binding. In fact, previous RR spectra of the WT showed that the heme propionate deformation mode changes from 376 cm^{-1} in the reduced form to 383 cm^{-1} in the O_2-bound form, meaning that the propionate side chains are significantly influenced upon O_2 binding.[32] Admittedly, the crystal structures of the reduced and O_2 forms of the WT show that both propionate side chains of heme rotate upon the ligand switch from Met95 to O_2.[18] The rotation of the 7-propionate side chain is accompanied by rearrangement of the hydrogen-bonding network including Arg97 and heme-bound O_2.[18] We suggest that the rotation of the 6-propionate side chain may trigger the formation of the hydrogen bond between Asn84 (F-helix) and Tyr126 (I_β sheet) through the heme 6-propionate hydrogen-bonding network (Figure 1B) in the O_2-bound form.

Furthermore, it was reported previously that the Asp40−Arg85 salt bridge of *Ec* DOS was important for the catalytic control, where the cleavage of this salt bridge by mutations of Asp40 abolished the PDE activity toward cAMP.[33] Since Arg85 is located in the immediate neighborhood of Asn84 and also contacts Tyr126,[18] the alteration in the heme 6-propionate hydrogen-bonding network may communicate the conformational changes from the F-helix to the I_β strand on the surface of the sensor domain. Consistent with this idea, the PDE activities for the ligand bound forms of N84V and Y126F mutants toward c-di-GMP examined in the present study are decreased by ∼46 to 68% compared to that of the WT. Therefore, we propose that a part of the conformational changes that occur in the sensor domain upon O_2- (or CO-) binding is propagated to the C-terminal PDE domain through the heme 6-propionate hydrogen-bonding network, bringing about regulation of the enzymatic activity.

Heme Discriminates among Different Ligands. The kinetics for O_2 and CO binding to the heme demonstrated that the WT *Ec* DOSH discriminates strongly against CO.[9,34] In addition, the ν_{Fe-O_2} frequency of *Ec* DOSH (561 cm^{-1}) is considerably

(29) Matsuno, M.; Takeuchi, H. *Bull. Chem. Soc. Jpn.* **1998**, *71*, 851−857.
(30) Kurokawa, H.; Lee, D.-S.; Watanabe, M.; Sagami, I.; Mikami, B.; Raman, C. S.; Shimizu, T. *J. Biol. Chem.* **2004**, *279*, 20186−20193.
(31) Crosson, S.; Rajagopal, S.; Moffat, K. *Biochemistry* **2003**, *42*, 2−10.
(32) Sato, A.; Sasakura, Y.; Sugiyama, S.; Sagami, I.; Shimizu, T.; Mizutani, Y.; Kitagawa, T. *J. Biol. Chem.* **2002**, *277*, 32650−32658.
(33) Watanabe, M.; Kurokawa, H.; Yoshimura-Suzuki, T.; Sagami, I.; Shimizu, T. *Eur. J. Biochem.* **2004**, *271*, 3937−3942.

low,[32,35] in agreement with the crystal structure that indicates Arg97 forms hydrogen bonds with bound O_2.[18] On the other hand, the RR spectrum of ν_{CO} of *Ec* DOSH (1972 cm^{-1}) indicated the absence of the hydrogen-bonding interaction of the heme-coordinated CO and the surrounding residues.[32,35] Thus, the hydrogen bonding interactions of the heme-bound gaseous ligand with the surrounding residues such as Arg97 is probably crucial for ligand discrimination and therefore, the heme-bound CO is discriminated from heme-bound O_2. These observations are compatible with the present results in which heme discriminates between O_2 and CO, resulting in different conformational changes in the protein moiety of *Ec* DOSH. Specifically, the UVRR results show that the environment around Trp53 changes toward more hydrophobic upon O_2 binding, while toward more hydrophilic upon CO-binding. In addition, Tyr55 that is located near Trp53, experiences no environmental changes upon O_2-binding, whereas it undergoes appreciable changes upon CO-binding.

Furthermore, the redox change of the heme iron induces some conformational changes which are significantly different from those observed upon O_2 or CO binding. For instance, no significant alteration in the heme 6-propionate hydrogen-bonding network is observed upon heme oxidation,[30] where a water molecule (or hydroxide anion) is the axial ligand of iron in the distal side of the heme.[30] The results suggest that heme can discriminate between exogenous gaseous (O_2 and CO) and solvent (water) ligands.

(34) Taguchi, S.; Matsui, T.; Igarashi, J.; Sasakura, Y.; Araki, Y.; Ito, O.; Sugiyama, S.; Sagami, I.; Shimizu, T. *J. Biol. Chem.* **2004**, *279*, 3340−3347.
(35) Gonzalez, G.; Dioum, E. M.; Bertolucci, C. M.; Tomita, T.; Ikeda-Saito, M.; Cheesman, M. R.; Watmough, N. J.; Gilles-Gonzalez, M.-A. *Biochemistry* **2002**, *41*, 8414−8421.

Conclusions

Our UVRR investigation of the ligand-bound (O_2 and CO) forms of WT and variants *Ec* DOSH has brought new insights into the structural basis of ligand differentiation by this heme sensor. In particular, it has revealed the importance of contact interactions between Trp53 and the 2-vinyl group of the heme. Furthermore, the UVRR results demonstrate the occurrence of a large change in the heme 6-propionate hydrogen-bonding network upon ligand binding. Specifically, Asn84 forms a hydrogen bond with Tyr126 in the O_2 and CO bound forms but not in the simply reduced form. Moreover, the PDE activities of the ligand bound forms for N84V and Y126F mutants are significantly reduced in comparison with that of the WT. These results explicitly show for the first time the role of the hydrogen-bonding network starting from the 6-propionate of heme in communicating the conformational changes of the heme to the protein moiety in *Ec* DOS.

Acknowledgment. We thank Dr. Takeshi Uchida for stimulating discussion. This study was supported by a fellowship to S.F. E.-M. from the Japan Society for the Promotion of Science and by a Grant-in-Aid for Specifically Promoted Research to T.K. (14001004) from the Ministry of Education, Culture, Sports, Science and Technology.

Supporting Information Available: Figures S1−S4 and the method of expression and purification for *Ec* DOS protein. This material is available free of charge via the Internet at http://pubs.acs.org.

JA0669777